CrossMark

ORIGINAL PAPER

Astrocyte Transcriptome from the Mecp2[308]-Truncated Mouse Model of Rett Syndrome

Chloé Delépine[1,2,3] · Juliette Nectoux[1,2,3,4] · Franck Letourneur[1,2,3] ·
Véronique Baud[1,2,3] · Jamel Chelly[1,2,3] · Pierre Billuart[1,2,3] · Thierry Bienvenu[1,2,3,4]

Abstract Mutations in the gene encoding the transcriptional modulator methyl-CpG binding protein 2 (MeCP2) are responsible for the neurodevelopmental disorder Rett syndrome which is one of the most frequent sources of intellectual disability in women. Recent studies showed that loss of Mecp2 in astrocytes contributes to Rett-like symptoms and restoration of Mecp2 can rescue some of these defects. The goal of this work is to compare gene expression profiles of wild-type and mutant astrocytes from Mecp2[308/y] mice (B6.129S-MeCP2<tm1Heto>/J) by using Affymetrix mouse 2.0 microarrays. Results were confirmed by quantitative real-time RT-PCR and by Western blot analysis. Gene set enrichment analysis utilizing Ingenuity Pathways was employed to identify pathways disrupted by Mecp2 deficiency. A total of 2152 genes were statistically differentially expressed between wild-type and mutated samples, including 1784 coding transcripts. However, only 257 showed fold changes >1.2. We confirmed our data by replicative studies in independent primary cultures of cortical astrocytes from Mecp2-deficient mice. Interestingly, two genes known to encode secreted proteins, chromogranin B and lipocalin-2, showed significant dysregulation. These proteins secreted from Mecp2-deficient glia may exert negative non-cell autonomous effects on neuronal properties, including dendritic morphology. Moreover, transcriptional profiling revealed altered Nr2f2 expression which may explain down- and upregulation of several target genes in astrocytes such as Ccl2, Lcn2 and Chgb. Unraveling Nr2f2 involvement in Mecp2-deficient astrocytes could pave the way for a better understanding of Rett syndrome pathophysiology and offers new therapeutic perspectives.

Keywords Transcriptome · Astrocyte · Mecp2 · Rett syndrome · NF-κB pathway · Nr2f2

✉ Thierry Bienvenu
thierry.bienvenu@inserm.fr

1 Inserm, U1016, Faculté de Médecine, Laboratoire de Génétique et de Physiopathologie des Maladies Mentales, Institut Cochin, 24 Rue du Faubourg Saint Jacques, 75014 Paris, France

2 Cnrs, UMR8104, Paris, France

3 Université Paris Descartes, Sorbonne Paris Cité, Paris, France

4 Groupe Universitaire Paris Centre, Site Cochin, Laboratoire de Biochimie et Génétique Moléculaire, Assistance Publique - Hôpitaux de Paris, 27 rue du Faubourg Saint Jacques, 75014 Paris, France

Introduction

Mutations in the gene encoding the methyl-CpG binding protein 2 (MeCP2) are implicated in the postnatal neurodevelopmental disorder Rett syndrome (RTT, MIM 312750), and 90 % of classical RTT patients carry *MECP2* mutations (Amir et al. 1999). This genetic disease is characterized by a normal postnatal development for the first few months followed by developmental stagnation and regression, loss of purposeful hand movements and speech, *autistic*-like behaviors, truncal ataxia, stereotypic hand movements, deceleration of brain growth, autonomic dysfunction and seizures (Bienvenu and Chelly 2006).

MeCP2 is a member of the methyl-CpG binding protein family and is composed by three domains: the methyl-binding domain (MBD), the transcriptional repression

domain (TRD) and a C-terminal domain, in addition to two nuclear localization signals (NLS). The MBD specifically binds to methylated CpG dinucleotides, with high affinity for CpG sequences with adjacent A-/T-rich motifs (Klose et al. 2005), but also binds to unmethylated four-way DNA junctions with a similar affinity, indicating a role of MeCP2 in higher-order chromatin interaction (Bienvenu and Chelly 2006). The function of MeCP2 as a transcriptional repressor was first suggested based on in vitro experiments. However, more recent studies suggest that MeCP2 regulates the expression of a wide range of genes and that it can both repress and activate transcription (Yasui et al. 2007; Chahrour et al. 2008).

Given that RTT may likely result from dysfunction of a transcriptional modulator activity of MeCP2, several groups have developed strategies to identify the transcriptional targets of MeCP2 in order to gain insight into the disease pathogenesis. The majority of these transcriptional profiling studies have been performed using total or specific brain tissue from Mecp2-null mice and RTT patients (Horike et al. 2005; Bienvenu and Chelly 2006; Yasui et al. 2007; Chahrour et al. 2008).

However, several recent studies showed that MeCP2 is clearly detected by immunostaining in all glial cell types including astrocytes, oligodendrocyte progenitor cells and oligodendrocytes, based on costaining for the cell-specific markers (GFAP, NG2 and myelin), respectively (Ballas et al. 2009; Maezawa et al. 2009; Nguyen et al. 2013). Using an in vitro coculture system, it has been shown that mutant astrocytes from a RTT mouse model and their conditioned medium fail to support normal dendritic morphology of either wild-type or mutant hippocampal neurons (Ballas et al. 2009). Although defective neurons clearly underlie the aberrant mice behaviors, these data suggested that the loss of MeCP2 from glia negatively influences neurons in a non-cell autonomous fashion (Ballas et al. 2009). In MeCP2-deficient mice, re-expression of *Mecp2* preferentially in astrocytes significantly improved locomotion and anxiety levels, restored respiratory abnormalities to a normal pattern, and greatly prolonged lifespan compared to globally null mice. Furthermore, restoration of MeCP2 in the mutant astrocytes exerted a non-cell autonomous positive effect on mutant neurons in vivo, restoring dendritic morphology and increasing levels of the VGLUT1 transporter (Lioy et al. 2011). Finally, it has been shown that Mecp2 is involved the differentiation of neural progenitors into astrocytes (Andoh-Noda et al. 2015). These data showed that glia, like neurons, are integral components of the neuropathology of RTT.

In the present study, we analyzed expression profiling by studying astroglial cultures from male wild-type and Mecp2-deficient mice. We choose to study Mecp2[308/y]

mice. In this mouse model Mecp2[308], a premature stop codon was inserted after codon 308 of the *Mecp2* gene and Mecp2[308/y] mice express a non-functional truncated protein, like approximately 50 % of RTT patients (Shahbazian et al. 2002). This truncated protein may bind promoter of several target genes. However, inability to phosphorylate the truncated Mecp2 protein at position 308 and 421 may affect the ability of Mecp2 to modulate transcription (Ebert et al. 2013). These mice develop milder symptoms than Mecp2-null mice but show RTT-like phenotypes, including stereotypic limb movements, and impairments in social and spatial memory (Shahbazian et al. 2002; De Filippis et al. 2010).

Materials and Methods

Animals

The animals used are Mecp2[308] and wild-type littermates (B6.129S-MeCP2<tm1Heto>/J, stock number: 005439; backcrossed to C57BL/6J mice for at least 12 generations from the Jackson Laboratories, USA). All procedures were carried out in accordance with the new European Communities Council Directive (2010/063 EU) and the implementing French decree of application n° 2013-118 01 and its supporting annexes entered into legislation February 01, 2013. All procedures were formally approved by local ethical committee from Paris Descartes University. Mice were housed at the Institut Cochin animal facility in groups of 3–6 in polycarbonate transparent, 530 cm², cages with corncob bedding and filtered air. Animals are kept on 12-h light–dark schedule (lights off at 7:00). Temperature was maintained at 21 °C ± 1 °C and relative humidity at 55 % ± 10 %. Animals were provided ad libitum with water and a complete pellet diet (SAFE, Paris, France).

Preparation of Primary Cultures of Astrocytes

Newborns at postnatal day zero (day of birth, P0) resulting from crossing Mecp2[308/+] heterozygous female with wild-type male mice were used for the preparation of dissociated cortical cell cultures. Primary astrocyte cultures were prepared from Mecp2[308/y] and wild-type males' cerebral cortex according to previously described methods (Gebicke-Haerter et al. 1989). Briefly, brains were dissected, cortices were isolated from the ventral telencephalon, and the tissue was mechanically dissociated following incubation at 37 °C for 30 min in 0.05 % trypsin. Dissociated cells were resuspended in DMEM with 10 % FBS. The resulting cultures were composed of more than 95 % astrocytes (as determined by immunoreactivity for GFAP).

Immunostaining

Cells were washed twice with PBS and fixed with methanol at -20 °C during 7 min, incubated with appropriated antibodies (anti-GFAP, Santa Cruz sc-6170) and then mounted with Fluoromount mounting medium with DAPI (Sigma-Aldrich, St. Louis, MO, USA) and analyzed with a Leica DMRA2 fluorescence microscope.

Microarray Data Analysis

Seven days in vitro confluent astrocytes cultures from four wild-type and four mutant mice, all littermates, were used for total RNA extraction with the Qiagen RNeasy kit (Qiagen, Courtaboeuf, France) as described by the manufacturer. Total RNA from each primary astrocyte culture was analyzed with the Affymetrix Mouse 2.0 Chips (a genome-wide array with 54,674 probe sets). RNA was scanned for purity, quality and amount with an Agilent 2100 Bioanalyzer using the RNA 6000 Nano LabChip®. When the 18S/28S ratio was ∼2.0, total RNA was subjected to subsequent labeling and cDNA synthesis for hybridization was carried out with 2 µg of total RNA and standard Affymetrix kits (Affymetrix, High Wycombe, UK). cDNA was washed with the Affymetrix cDNA cleanup kit. In vitro transcription and labeling of cRNA were performed with Affymetrix reagents designed for in vitro transcription, amplification and biotin labeling to generate targets for GeneChip® brand arrays. Hybridization was carried out according to the Affymetrix Gene-Chip® Manual. Fifteen micrograms of labeled, fragmented in vitro transcription material was the nominal amount used on the GeneChip® arrays. The arrays were incubated 16 h at a constant 45 °C temperature. Preparation of microarrays was carried out with Affymetrix wash protocols in a Model 450 Fluidics station under the control of Affymetrix Gen-eChip Operating Software. Scanning was carried out with an Affymetrix Model 3000 scanner with an autoloader.

Fluorescent data were exported to two complementary analysis packages: (1) Genespring software (Agilent Technologies) with GC-RMA algorithm for data normalization; and (2) R Bioconductor with the Robust Multichip Average (RMA) module with MAS5.0 algorithm for data filtering (http://www.r-project.org/). Normalization by Genespring GC-RMA allows a model-based probe-specific background correction to maintain accuracy even for very low expressed genes (Irizarry et al. 2006). MAS5.0 detection flags allow accuracy in signal quality filtering. It generates a p-score that assesses the reliability of each expression level, considering the significance of the differences between the perfect match (PM) and the mismatch values (MM) for each probeset. One of the following flag—"absent," "marginal" or "present"—is associated with each probe pair according to the strength of the fluorescent signal. For statistical analyses, differences in gene expression level between all wild-type and mutant cultures were calculated. To estimate the false discovery rate, the resulting p values were corrected by the Benjamini and Hochberg method. Cluster analysis was performed by hierarchical clustering in Genespring using the Spearman correlation similarly measure and average linkage algorithm.

Ingenuity Analysis

Pathways, upstream regulators and functional enrichment analysis were carried out through the use of IPA software (Ingenuity® Systems, USA, www.ingenuity.com).

Quantitative Real-Time PCR

Total RNA from the eight astroglial cultures was converted to cDNA with Maxima First Strand cDNA synthesis Kit (ThermoScientific, Rochester, USA) for quantitative real-time PCR with SYBR Green as detection agent with the LightCycler480 detection system (Roche Applied Bioscience, Indianapolis, IN, USA). Primer sequences are described in Table 1. After PCR amplification, a dissociation protocol was performed to determine the melting curve of the PCR product. Reactions with melting curves indicating a single amplification product were considered positive for further analysis. The identity and expected size of the single PCR product were also confirmed by agarose gel electrophoresis. For each cycle, a relative quantification of the amount of each individual gene was calculated by the comparative $\Delta\Delta CT$ method as described by the manufacturer, providing a relative measure of the expression of the genes of interest, which were all normalized. Normalization factor was based on the geometric mean of control gene *GAPDH* and *cyclophilin*. Statistical analysis was carried out using the nonparametric Mann–Whitney test. A p value <0.05 was considered as significant.

Replicative Studies

To confirm data obtained by microarray analysis, total RNA from additional independent astrocyte cultures was converted to cDNA for quantitative real-time PCR with SYBR Green as described above. As biological replicates, a total of fourteen Mecp2$^{308/y}$ and eleven wild-type P0 newborns from seven distinct litters were used. Each litter was composed of at least one mutant and one wild-type males. Primary astrocyte cultures from one litter represent one independent experiment. As experiment itself could be a source of variation, statistical analysis was performed

Table 1 Sequences of forward and reverse primers used for quantitative real-time RT-PCR

Gene	Primer Fd	Primer Rv
Adcy8	TCACAGAAGGATCGTGGAGC	GTGCGAGATGGTTTGGAAGC
Basp1	GGAGAGAGAGAGAGCCTTTGCTG	TTCTTGCTCAGCTTGCCTCC
Cdon	TGGATTCATGCAGTCTACTGGG	ACAAAGTCTCCATCCATCACCT
Chgb	CCGGCAAGTCCTGAAGAAGA	CATCGGCTGGGTCTCTTAGC
Ccl2	TCACCAGCAAGATGATCCCAA	GCACAGACCTCTCTCTTGAGC
Eif4a2	TGACGTGCAACAAGTGTCCT	TTTCCTCCCAAATCGACCCC
Gad1	ACTCAGCGGCATAGAAAGGG	GAAGAGGTAGCCTGCACACA
Gga1	GTGTCCCTGCTTGATGACGA	GACTGGAAGTTGTCCCACCC
Grid2	TATGTTGCACCGGACCACAA	TTCTCCCGGTCTGGAGTGAT
Htr5b	GGTGGTGCTCTTCGTCTACTG	GGGCTGTGAACACCATCTCAG
Lcn2	TACAATGTCACCTCCATCCTGG	TGCACATTGTAGCTCTGTACCT
Myoc	TTCCACCCAGTACCCCTCTC	TTGGGAAGCAGGAACCTCAG
Nr2f2	CGGAGGAACCTGAGCTACAC	AGGCATCCTGCCTCTCTGTA
Prkcq	ACTTTGACTGTGGGACCTGC	GGTGGGTACATGGTTGGCTT
Shh	TGGAAGCAGGTTTCGACTGG	GAAACAGCCGCCGGATTTG
Slc17a8	GGGATGTGGAGTAAGTGGGC	TACTGCACCAATACCCCTGC

using two-way ANOVA test with genotype and experiment as variables. A p value <0.05 was considered as significant.

Western Blot

The levels of NR2F2, CHGB, MYOC and CDON protein expression from three pairs of wild-type and Mecp2-deficient littermate pups were determined by Western blot analysis. Briefly, proteins were extracted from astrocyte cultures in RIPA buffer supplemented with protease inhibitors (Sigma-Aldrich). The protein samples were separated by a 10 % sodium dodecyl sulfate–polyacrylamide gel electrophoresis and then transferred to Hybond-C nitrocellulose membrane (GE Health care, Piscataway, NJ). After blocking nonspecific sites by a TBS-Tween 20 0.05 %/5 % fat milk solution for 1 h at room temperature, the membrane was incubated overnight at 4 °C with a rabbit anti-COUP-TFII polyclonal antibody (kindly provided by Mireille Cognet-Vasseur, Institut Cochin, dilution 1:1000), a goat anti-chromogranin B polyclonal antibody (Santa Cruz Biotechnology, dilution 1:100), a mouse anti-CDON polyclonal antibody (R&D systems, dilution 1:100) washed and incubated, respectively, with horseradish peroxidase (HRP)-conjugated secondary antibodies (anti-rabbit, anti-mouse or anti-goat, dilution 1:5000), and developed with the enhanced chemiluminescence method (ECL; GE Healthcare). We also probed membranes for GAPDH (antibody anti-GAPDH Ambion, dilution 1:1000) for loading normalization. Quantification of protein levels was measured by the chemiluminescence intensity. Normalized protein levels were analyzed with the nonparametric Mann–Whitney test. A p value <0.05 was considered as significant.

Electrophoretic Mobility Shift Assay (EMSA)

Monolayers of astrocytes were washed with PBS, and proteins were extracted with buffer containing 20 mM HEPES (pH 7.9), 0.4 mM NaCl, 1.0 mM EDTA, 1.0 mM EGTA, 1.0 mM DTT and 1.0 mM phenylmethylsulfonyl fluoride. Insoluble material was removed by centrifugation at 14,000 rpm, and the supernatant containing the proteins was stored at—80 °C until use. EMSA was performed using gel shift assay system (Promega, Madison, WI, USA) (Jacque et al. 2005). The HIV-LTR tandem κB oligonucleotide was end labeled by T4 polynucleotide kinase using [γ-32P]-ATP (PerkinElmer) and used as κB probe (Authier et al. 2014). Fifteen micrograms of total protein extracts was incubated at room temperature for 40 min in 20 μL binding buffer (10 mM Tris–HCl (PH 7.6), 100 mM NaCl, 2 % glycerol, 1 mM EDTA, 5 mM DTT and 3,7 μg poly dI-dC) containing 0.5 μL of ^{32}P-labeled oligonucleotide κB probe. The DNA–protein complexes were separated by electrophoresis on 5 % nondenaturing polyacrylamide gel in 0.25 × TBE buffer (tris–borate–EDTA) at 170 V for 90 min. After electrophoresis, the gel was dried and exposed to X-ray film. The unbound probe was used as a loading control. Two litters were used in two independent experiments (two wild-type and one Mecp2-deficient male newborn pups in experiment 1, and two wild-type and four Mecp2-deficient male newborn pups in experiment 2).

RNA Interference

Three independent experiments were performed on primary astrocyte cultures from newborn P0 wild-type pups, each time with two biological replicates by genotype. To deplete

Nr2f2 expression, ON-TARGET™ small interfering RNA (siRNA) from Dharmacon (GE Health care, Piscataway, NJ, USA) was used (pool of four siRNA, target sequences: 5′-CAGCCAACACGGUUCGGAA-3′, 5′-GCUUUGGAAGA GUACGUUA-3′, 5′-GGAGCGAGCUGUUCGUGUU-3′, 5′-GUACCUGUCCGGAUAUAUU-3′). As a negative control, we used Dharmacon's ON_TARGET™ nontargeting siRNA pool. Cells were transfected with 20 nM of siRNA with Lipofectamine LTX reagent (Life Technologies), according to the manufacture's instructions. Statistical analysis was carried out using the nonparametric Mann–Whitney test. A p value <0.05 was considered as significant.

Results

Microarray Analysis of Wild-Type and Mecp2-Mutant Astrocytes

Gene expression of primary cultures of astrocytes from four wild-type and four mutant P0 pups, all littermates, was analyzed by microarray. Hybridizations of labeled RNA on Affimetrix Mouse 2.0 chips were carried out in technical duplicate for each astrocytes culture. Signals of all hybridized chips were normalized using the GC-RMA method. Microarray data have been submitted into the GEO database (http://www.ncbi.nlm.nih.gov/geo/query/acc.cgi?to ken=czslkgwclzezvep&acc=GSE56709). t test analysis, considering a $p < 0.05$, yielded a total of 2152 coding and uncoding genes with significantly different expression between wild-type and mutant samples. Of these, 1784 were coding genes. t test analysis, considering also a 1.20-fold expression variation, yielded a total of 257 genes. A total of 132 genes were overexpressed, and 125 were underexpressed in mutant astrocytes compared to wild-type astrocytes (Supp. Info. Table S1).

Validation of Microarray Data by Quantitative RT-PCR Analysis of Wild-Type and Mecp2-Mutant Astrocytes

Among the most dysregulated transcripts, we focused on a selection of 16 candidate genes based on both fold-change value, significative expression level and functional relevance (Colantuoni et al. 2001; Ben-Shachar et al. 2009; Yasui et al. 2013). To assess the reliability of the microarray results, transcript levels of those 16 differentially expressed genes (*Adcy8*, *Cdon*, *Chgb*, *Gga1*, *Grid2*, *Htr5b*, *Myoc*, *Prkcq* and *Slc17a8* with increased expression and *Basp1*, *Ccl2*, *Eif4a2*, *Gad1*, *Lcn2*, *Nr2f2* and *Shh* with decreased expression) were quantified using real-time quantitative RT-PCR analysis with SYBR Green®. The same RNA samples used for making array hybridization probes were used as

templates for RT-PCR. The Pearson correlation coefficient was 0.6254 (p value <0.05) (Fig. 1a).

Importantly, to confirm our data, we performed replicative studies using other independent astroglial cultures. A total of fourteen Mecp2[308/y] and eleven wild-type P0 newborns from seven distinct litters were used. Each litter was composed at least of one mutant and one wild-type males. As previously shown (Yasui et al. 2013), we observed high inter-individual biological variations. Nevertheless, we found five transcripts significantly increased in Mecp2[308/y] astrocytes (*Adcy8*, *Cdon*, *Chgb*, *Htr5b* and *Myoc*) and five transcripts significantly decreased in Mecp2[308/y] astrocytes (*Ccl2*, *Gad1*, *Lcn2*, *Nr2f2* and *Shh*) (Table 2). Although more data may be necessary to have significant statistic values, *Basp1* expression level tends to be decreased as it was shown by the microarray assay. In contrast, no significant alteration in *Gga1* and *Slc17a8* transcript's level was observed in this replicative experiment (Table 2). Finally, change in mRNA expression level of selected genes found in this replicative study significantly correlate with the microarray data, assessing the reproducibility of those results. Pearson correlation coefficient was 0.99 (p value <0.001) (Fig. 1b).
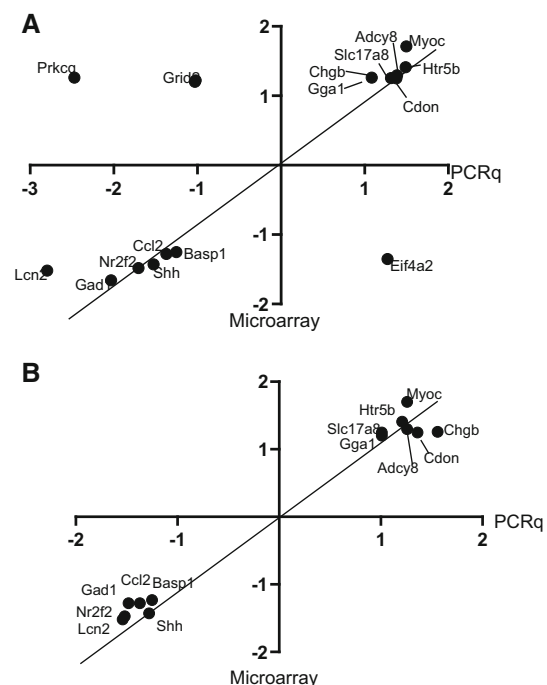

Fig. 1 a Correlation diagram between quantitative RT-PCR results and microarray data from the same total RNA extracted from primary cultures of Mecp2-deficient (Mecp2[308/y]) and wild-type (Mecp2[WT/y]) astrocytes. The Pearson correlation coefficient was 0.6254 (p value <0.05). b Correlation diagram between quantitative RT-PCR results and microarray data from total RNA extracted from seven independent primary cultures of Mecp2-deficient (Mecp2[308/y]) and wild-type (Mecp2[WT/y]) astrocytes. Fold-change values of gene expression level in Mecp2-deficient astrocytes over WT astrocytes are plotted. *Line* represents the theoretical correlation. The Pearson correlation coefficient was 0.99 (p value <0.05)

Table 2 Gene expression fold changes in Mecp2-deficient (Mecp2$^{308/y}$) versus wild-type (Mecp2$^{WT/y}$) astrocytes obtained from replicative studies

Gene symbol	Gene name	fold change	p value
Adcy8	Adenylate cyclase 8	1.26	**0.046**
Basp1	Brain abundant, membrane attached signal protein 1	−1.25	0.066
Ccl2	Chemokine (C–C motif) ligand 2	1.36	**0.001**
Cdon	Cell adhesion molecule related/downregulated by oncogenes	1.56	**0.002**
Chgb	Chromogranin B	−1.37	**0.001**
Gad1	Glutamate decarboxylase 1	−1.48	**0.001**
Gga1	Golgi associated, gamma adaptin ear containing, ARF binding protein 1	1.01	0.556
Htr5b	5-Hydroxytryptamine (serotonin) receptor 5B	1.21	**0.002**
Lcn2	Lipocalin 2	−1.54	**0.001**
Myoc	Myocilin	1.26	**0.001**
Nr2f2	Nuclear receptor subfamily 2, group F, member 2	−1.52	**0.001**
Shh	Sonic hedgehog	−1.28	**0.001**
Slc17a8	Solute carrier family 17 (sodium-dependent inorganic phosphate cotransporter), member 8	1.01	0.421

Significant p values are given in bold

Normalization factor was based on the geometric mean of control gene *GAPDH* and *cyclophilin*

Protein Expression of Dysregulated Genes *Cdon, ChgB, Myoc* and *Nr2f2* in Mecp2-Deficient Astrocytes

Among the dysregulated genes validated by microarray and quantitative RT-PCR, we analyzed by Western blot the protein expression for CDON, CHGB, MYOC and NR2F2 in three independent experiments composed of pairs of wild-type and Mecp2-deficient littermate pups. Significant overexpression of *Cdon* mRNA was confirmed at the protein level (Fig. 2). On the other hand, although *Nr2f2* mRNA level was found to be downregulated in the Mecp2-deficient astrocytes, we found a significant overexpression of NR2F2 protein in three independent experiments. Results may be explained by the fact that NR2F2 is a transcription factor able of a negative feedback on its own transcription (Boutant et al. 2012). Similarly, although *Chgb* mRNA level was upregulated in Mecp2-deficient astrocytes, CHGB protein level was significantly down-regulated in three independent experiments (Fig. 2). Although *Myoc* mRNA level was found upregulated in Mecp2-deficient astrocytes, no significant difference in myocilin protein level was found between wild-type and Mecp2-deficient astrocytes.

IPA Analysis Identified Cellular Functions and Pathways Significantly Enriched in the List of Mecp2-Deficient Astrocytes Dysregulated Genes

The microarray data of the 257 significantly dysregulated genes were analyzed with IPA software. IPA software identified four IPA molecular and cellular functions significantly enriched in our list of dysregulated genes:

cellular development (p value 1.42E−04, 33 genes), cell morphology (p value 1.74E−04, 19 genes), cell-to-cell signaling and interaction (p value 1.71E−04, 13 genes), and cellular growth and proliferation (p value 5.72E−04, 25 genes). Moreover, some Ingenuity Canonical Pathways were significantly enriched in our 257 genes list. The most significant pathways were complement system (p value 0.015; ratio 0.059), glutamate receptor signaling (p value 0.043; ratio 0.032) and cytokine signaling (p value 7.76E−03; ratio 0.087).

Several Potential NF-κB Target Genes are Dysregulated in Mecp2-Deficient Astrocytes Independently of NF-κB Pathway

As shown in Fig. 3a, the 257 dysregulated genes list was significantly enriched in NF-κB targets (IPA Upstream Regulators Analysis, activation z-score 1.571, p value of overlap 0.016). NF-κB (nuclear factor kappa-light-chain-enhancer of activated B cells) is a protein complex that controls transcription of DNA, either repressing or activating gene expression. Interestingly, four of NF-κB targets were already emphasized in our qRT-PCR replicative studies (*Ccl2*, *Gad1*, *Lcn2* and *Shh*). To study the potential NF-κB activity dysregulation, we evaluated the NF-κB DNA binding activity in cell nuclear extracts by EMSA. Results did not show a significant variation in NF-κB complexes DNA binding activity in protein extracts of Mecp2-deficient astrocytes in comparison with wild-type ones (Fig. 3b). These data suggest that the underexpression of *Ccl2*, *Gad1*, *Lcn2* and *Shh* genes in Mecp2-deficient astrocytes was not due to NF-κB pathway dysregulation.

Fig. 2 CDON, CHGB, MYOC
and NR2F2 protein expression
levels determined by Western
blot analysis in Mecp2-deficient
(Mecp2$^{308/y}$) and wild-type
(Mecp2$^{WT/y}$) astrocytes. *Bars*
represent the relative
quantification of protein levels
measured with the
chemiluminescence intensity.
Normalization factor was based
on control protein GAPDH
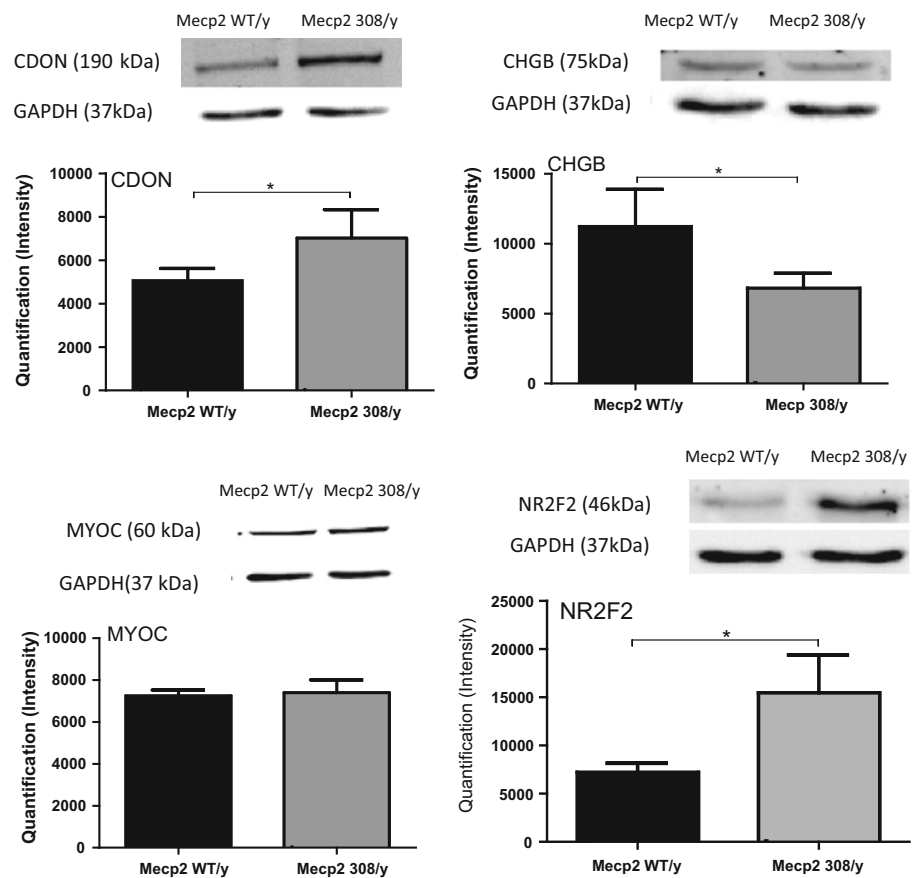
Nr2f2 Silencing and Mecp2 Deficiency in Astrocytes Causes Similar mRNA Expression Changes

Nuclear receptor subfamily 2, group F, member 2 (NR2F2)
is a transcription factor able of acting as both positive and
negative regulator which is required for gliogenic compe-
tence (Naka et al. 2008). Thus, we hypothesized that *Nr2f2*
mRNA downregulation in Mecp2-deficient astrocytes may
be involved in expression profile changes observed in our
transcriptomic analysis. To assess this hypothesis, we used
small interference RNA (siRNA) targeting *Nr2f2* expres-
sion in wild-type astrocytes and measured the effect on the
relative quantification of *Nr2f2, Adcy8, Ccl2, Cdon, Chgb,
Htr5b, Lcn2, Myoc* and *Shh* mRNA level by quantitative
RT-PCR. Three independent experiments were performed
on primary astrocyte cultures from newborn P0 wild-type
pups, each time with two biological replicates by genotype.
A reduction of 50 % of *Nr2f2* mRNA expression level,
similar to the downregulation of *Nr2f2* observed in Mecp2-
deficient astrocytes, was triggered after 24-h exposure to
the siRNA (Fig. 4). *Ccl2, Lcn2* and *Shh* mRNA levels were
downregulated, and *Adcy8, Cdon, Chgb, Htr5b, Myoc*
mRNA levels upregulated following the *Nr2f2* silencing.
Interestingly, a significant correlation was observed

considering the fold changes of mRNA expression between
Mecp2-deficient astrocytes and *Nr2f2* silencing experi-
ments (Pearson correlation coefficient of 0.79, *p* value
<0.05).

Discussion

Because initial immunohistochemical observations sug-
gested that MeCP2 was expressed exclusively in neurons,
the first studies suggested that Rett syndrome was due
exclusively to loss of MeCP2 function in neurons. How-
ever, several recent studies showed that MeCP2 is clearly
detected by immunostaining in all glial cell types including
astrocytes, oligodendrocyte progenitor cells and oligoden-
drocytes (Ballas et al. 2009; Maezawa et al. 2009; Nguyen
et al. 2013). Using an in vitro coculture system, it has been
shown that mutant astrocytes from a RTT mouse model
and from Rett syndrome patients-specific iPSCs fail to
support normal dendritic morphology of either wild-type or
mutant hippocampal neurons (Ballas et al. 2009; Maezawa
et al. 2009; Williams et al. 2014). Although defective
neurons clearly underlie the aberrant behaviors, these data
suggested that the loss of MeCP2 from glia negatively

A

Activation
Z-score : 1.57

NFkB

Ccl2   Lcn2   Shh   Gad1
-1.28   -1.52   -1.43   -1.28

Prediction Legend

☐ Downregulated

- - -> Leads to inhibition

B

Mecp2 WT/y   Mecp2 308/y
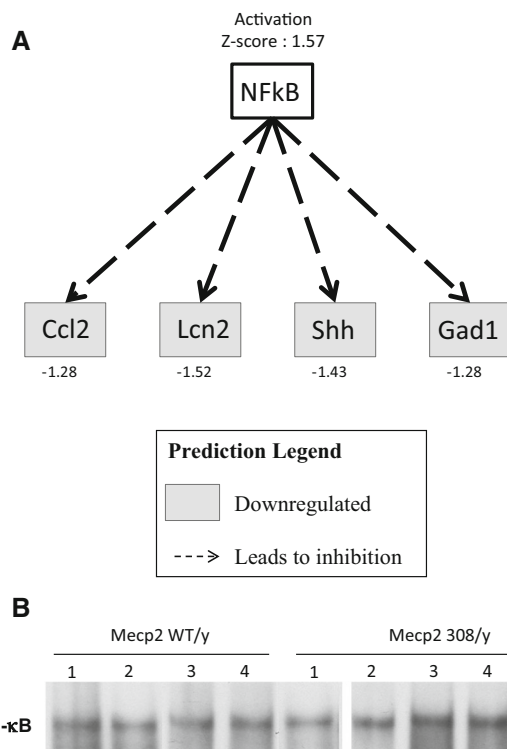
1   2   3   4   1   2   3   4   5

NF-κB

Fig. 3 **a** NF-κB pathway upregulation and downregulated target genes predicted by IPA software from the microarray dataset. *Gray rectangles* represent downregulated genes in Mecp2-deficient astrocytes in comparison with wild-type (WT) astrocytes. Number under the *rectangles* represents the gene expression fold change in Mecp2-deficient astrocytes over WT astrocytes. NF-κB pathway is predicted by IPA software to be activated in Mecp2-deficient astrocytes in comparison with WT astrocytes with an activation z-score of 1.57. **b** NF-κB complexes DNA binding activity in Mecp2-deficient (Mecp2$^{308/y}$) and wild-type (Mecp2$^{WT/y}$) astrocytes. Specific DNA binding of the NF-κB complexes is investigated using EMSA as described in Materials and Methods

influences neurons in a non-cell autonomous fashion (Ballas et al. 2009; Maezawa et al. 2009; Yasui et al. 2013). In Mecp2-deficient mice, re-expression of *Mecp2* preferentially in astrocytes significantly improved locomotion and anxiety levels, restored respiratory abnormalities to a normal pattern, and greatly prolonged lifespan compared to globally null mice (Lioy et al. 2011). These data showed that glia, like neurons, are integral components of the neuropathology of Rett syndrome.

In our study, we identified 257 genes affected by MeCP2 deficiency in astrocytes. The number of dysregulated genes and the level of mRNA expression changes were similar to those described in previous transcriptomic studies independently of cell or tissue models (Colantuoni et al. 2001; Ben-Shachar et al. 2009; Yasui et al. 2013). Among the identified target genes, 16 were selected for validation by quantitative RT-PCR. Indeed, functions of those genes were consistent with pathways affected in Rett syndrome
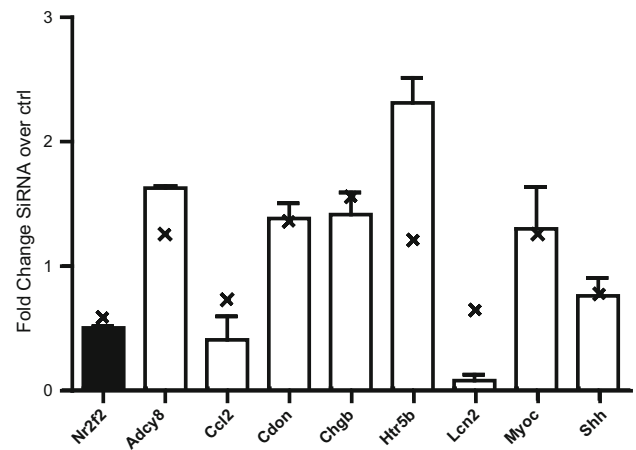
Fig. 4 *Nr2f2* gene expression silencing A. Relative *Nr2f2, Adcy8, Ccl2, Cdon, Chgb, Htr5b, Lcn2, Myoc* and *Shh* gene expression levels in wild-type astrocytes after 24 h of *Nr2f2* gene expression silencing. *Bars* represent the mean fold-change value of gene expression levels in wild-type astrocytes transfected 24 h with *Nr2f2* siRNA over gene expression levels in wild-type astrocytes transfected 24 h with nontargeting siRNA, ±SEM. *Crosses* represent the plotted fold-change values of gene expression level in Mecp2-deficient astrocytes over wild-type astrocytes obtained previously

and some may be involved in the non-cell autonomous effect on neurons. For those 16 genes, a strong correlation was found between the results of microarray and quantitative RT-PCR and between the microarray data and results obtained in replicative studies (Pearson correlation coefficient with p value <0.05 of 0.63 and 0.99, respectively). Our data compared with the other published report on Mecp2-deficient astrocytes in the literature display very limited overlap (Yasui et al. 2013). However, five common dysregulated genes were identified in both studies (Riken cDNA 3110003AA7, annexin A1, dihydropyrimidine dehydrogenase, lipocalin 2, and cell adhesion molecule related/downregulated by oncogenes, Cdon). The limited overlap of dysregulated genes identified in the two astroglial studies may have two main reasons: study of different mouse model (Mecp2$^{tm1;Bird+/y}$ and Mecp2$^{308y/-}$) and different number of cell division in vitro (astrocytes obtained from P0 mice after 2–4 weeks of in vitro culture vs 7 days of in vitro culture).

Recent studies showed that mutant astrocytes isolated from the Jaenisch MeCP2-knockout mice contribute to neuronal defects, probably as a result of aberrant secretion of soluble factor(s) (Ballas et al. 2009; Lioy et al. 2011). In this context, it is of interest to note that two secreted proteins, lipocalin 2 (LCN2) and Chromogranin B, a component of exocytose vesicles, are both dysregulated in Mecp2-deficient astrocytes.

LCN2 belongs to the lipocalin family, which is characterized by the ability to bind and transport lipids and

other hydrophobic molecules. Lcn2 is induced and secreted by reactive astrocytes. Interestingly, LCN2 has been shown to modulate spine morphology and to regulate neuronal excitability. As previously described by Ferreira and colleagues (Ferreira et al. 2013), LCN2-null mice displayed increased anxiety and depressive-like behaviors compared to wild-type controls as assessed by the decreased time they spent in the open arms of the elevated plus maze test and the decreased time spent in the light compartment of the light/dark box test when compared to wild-type mice (Ferreira et al. 2013).

In addition, LCN2-null mice presented synaptic impairment in hippocampal long-term potentiation (Ferreira et al. 2013). Our results suggest that LCN2 may be abnormally secreted by Mecp2-mutant astrocytes and may alter spine morphology and neuronal excitability on mutant as well as wild-type neurons. Further experiments need to be performed to characterize this aberrant secretion of LCN2 by Mecp2-deficient astrocytes. Unfortunately, because LCN2 shares homologous sequences with the 20 other lipocalin members, antibodies against LCN2 often recognize other lipocalin members (Bi et al. 2013). Very interestingly, lipocalin 2 was also observed as dysregulated in Mecp2-null astrocytes (Yasui et al. 2013), in postmortem brain from RTT patients (Colantuoni et al. 2001) and in total mice brain from Mecp2$^{tm1;Bird+/y}$ mice (Ben-Shachar et al. 2009).

The other dysregulated secreted protein is chromogranin B (previously called secretogranin I), an acidic protein consisting of single polypeptide chains that is mainly located within secretory vesicles such as chromaffin granules and large dense core vesicles of monoaminergic neurons. Chromogranin B has recently grown in importance after the unexpected finding associating it with some classes of human neurological diseases, such as schizophrenia (Landén et al. 1999; Marksteiner et al. 2000) and Alzheimer's disease (Marksteiner et al. 2000). Interestingly, chromogranin B is a highly efficient system directly involved in monoamine accumulation and in the kinetics of exocytosis from large dense core secretory vesicles (Díaz-Vera et al. 2010). Moreover, it is of interest to note that BDNF, the neurotrophic factor altered in Mecp2-deficient neurons, is known to be processed and secreted via secretory granule cargoes such as chromogranin B (Sadakata et al. 2004).

In line with previous studies, our transcriptional profiling revealed subtle changes in Mecp2-deficient astrocytes. However, IPA software analysis identified that the list of the 257 dysregulated genes in Mecp2-deficient astrocytes was significantly enriched in genes involved in major cellular functions such as cell–cell communication and cellular development in line with the non-cell autonomous effect of Mecp2-deficient astrocytes previously described

(Ballas et al. 2009). Moreover, as described by Yasui et al. 2013 for the Mecp2-null astrocytes, our list of dysregulated genes was significantly enriched in genes of the immune system, cytokine signaling and glutamate signaling, suggesting an impairment of specific astroglial functions (Ballas et al. 2009; Maezawa et al. 2009; Lioy et al. 2011). Interestingly, the finding of the enrichment in genes of glutamate signaling reinforces the data of Okabe and colleagues showing an alteration of glutamate clearance in astrocytes derived from an Mecp2-null mouse model of RTT (Okabe et al. 2012). Gene set enrichment analysis using Ingenuity Pathways identified the NF-κB pathway as significantly dysregulated. However, we were not able to confirm this by measurement of NF-κB DNA binding activity in Mecp2-deficient cultured astrocytes.

Interestingly, we identified the transcription factor NR2F2 (nuclear receptor subfamily 2, group F, member 2) as dysregulated in Mecp2-deficient astrocytes. NR2F2 (also known as NR2F1 and COUP-TFII) is a transcription factor able of acting as both positive and negative regulator which is required for gliogenic competence (Naka et al. 2008). In our study, Nr2f2 transcript was downregulated in the microarray data, whereas the protein was overexpressed in Mecp2-deficient astrocytes. Those data reinforce previous report suggesting a negative feedback of NR2F2 on its own transcription (Boutant et al. 2012).

Nr2f2 silencing in wild-type astrocytes induced a downregulation of Ccl2, Lcn2 and Shh genes and a upregulation of Adcy8, Cdon, Chgb, Htr5b, and Myoc genes. Interestingly, Nr2f2 silencing and Mecp2 deficiency in astrocytes cause similar mRNA expression changes considering our selected target genes. Our data may suggest that NR2F2 dysregulation may be involved in the pathophysiology of Rett syndrome. Indeed, NR2F2 has been reported to negatively regulate gene transcription by binding to the promoter and recruiting NCoR/SMRT corepressor complexes (Okamura et al. 2009). Moreover, it was found that MeCP2 is able to bind to those complexes (Lyst et al. 2013). These data suggest that NR2F2 and MeCP2 might regulate gene expression through common N-CoR/SMRT complexes. Missense mutations causing RTT may abolish protein interaction and contribute to gene expression dysregulation in astrocytes and RTT pathophysiology.

Conclusions

In summary, our study identified new genes as targets of MeCP2. Particularly, two genes encoding secreted proteins CHGB and LCN2 appeared to be interesting. These proteins secreted from MeCP2-deficient glia may exert negative non-cell autonomous effects on neuronal properties,

including dendritic morphology. Moreover, transcriptional profiling revealed altered *Nr2f2* expression which may explain down- and upregulation of several target genes in astrocytes such as *Ccl2*, *Lcn2* and *Chgb*. Our data suggest that unraveling NR2F2 involvement in Mecp2-deficient astrocytes could pave the way for a better understanding of Rett syndrome and offers a new therapeutic perspective.

References

Amir, R. E., Van den Veyver, I. B., Wan, M., Tran, C. Q., Francke, U., & Zoghbi, H. Y. (1999). Rett syndrome is caused by mutations in X-linked MECP2, encoding methyl-CpG-binding protein 2. *Nature Genetics, 23*, 185–188.

Andoh-Noda, T., Akamatsu, W., Miyake, K., Matsumoto, T., Yamaguchi, R., Sanosaka, T., et al. (2015). Differentiation of multipotent neural stem cells derived from Rett syndrome patients is biased toward the astrocytic lineage. *Molecular Brain, 27*, 31.

Authier, H., Billot, K., Derudder, E., Bordereaux, D., Rivière, P., Rodriguez-Ferreira, S., et al. (2014). IKK phosphorylates RelB to modulate its promoter specificity and promote fibroblast migration downstream to TNF receptors. *Proceedings of the National Academy of Sciences of USA, 111*, 14795–14799.

Ballas, N., Lioy, D. T., Grunseich, C., & Mandel, G. (2009). Non-cell autonomous influence of MeCP2-deficient glia on neuronal dendritic morphology. *Nature Neurosciences, 12*, 311–317.

Ben-Shachar, S., Chahrour, M., Thaller, C., Shaw, C. A., & Zoghbi, H. Y. (2009). Mouse models of MeCP2 disorders share gene expression changes in the cerebellum and hypothalamus. *Human Molecular Genetics, 18*, 2431–2442.

Bi, F., Huang, C., Tong, J., Qiu, G., Huang, B., Wu, Q., et al. (2013). Reactive astrocytes secrete lcn2 to promote neuron death. *Proceedings of the National Academy of Sciences of USA, 110*, 4069–4074.

Bienvenu, T., & Chelly, J. (2006). Molecular genetics of Rett syndrome: when DNA methylation goes unrecognized. *Nature Review Genetics, 7*, 415–426.

Boutant, M., Ramos, O. H., Tourrel-Cuzin, C., Movassat, J., Ilias, A., Vallois, D., et al. (2012). COUP-TFII controls mouse pancreatic β-cell mass through GLP-1-β-catenin signaling pathways. *PLoS ONE, 7*, e30847.

Chahrour, M., Jung, S. Y., Shaw, C., Zhou, X., Wong, S. T., Qin, J., & Zoghbi, H. Y. (2008). MeCP2, a key contributor to neurological disease, activates and represses transcription. *Science, 320*, 1224–1229.

Colantuoni, C., Jeon, H., Hyde, K., Chenchik, A., Khimani, A. H., Narayanan, V., et al. (2001). Gene expression profiling in postmortem Rett Syndrome brain: differential gene expression and patient classification. *Neurobiology of Diseases, 8*, 847–865.

De Filippis, B., Ricceri, L., & Laviola, G. (2010). Early postnatal behavioral changes in the Mecp2-308 truncation mouse model of Rett syndrome. *Genes Brain and Behaviour, 9*, 213–223.

Díaz-Vera, J., Morales, Y. G., Hernández-Fernaud, J. R., Camacho, M., Montesinos, M. S., Calegari, F., et al. (2010). Chromogranin B gene ablation reduces the catecholamine cargo and decelerates exocytosis in chromaffin secretory vesicles. *Journal of Neurosciences, 30*, 950–957.

Ebert, D. H., Gabel, H. W., Robinson, N. D., Kastan, N. R., Hu, L. S., Cohen, S., et al. (2013). Activity-dependent phosphorylation of MeCP2 threonine 308 regulates interaction with NCoR. *Nature, 499*, 341–345.

Ferreira, A. C., Pinto, V., Dá Mesquita, S., Novais, A., Sousa, J. C., Correia-Neves, M., et al. (2013). Lipocalin-2 is involved in emotional behaviors and cognitive function. *Frontiers Cell Neurosciences, 7*, 122.

Gebicke-Haerter, P. J., Bauer, J., Schobert, A., & Northoff, H. (1989). Lipopolysaccharide-free conditions in primary astrocyte cultures allow growth and isolation of microglial cells. *Journal of Neurosciences, 9*, 183–194.

Horike, S., Cai, S., Miyano, M., Cheng, J. F., & Kohwi-Shigematsu, T. (2005). Loss of silent chromatin looping and impaired imprinting of DLX5 in Rett syndrome. *Nature Genetics, 37*, 31–40.

Irizarry, R. A., Wu, Z., & Jaffee, H. A. (2006). Comparison of Affymetrix genechip expression measures. *Bioinformatics, 22*, 789–794.

Jacque, E., Tchenio, T., Piton, G., Romeo, P. H., & Baud, V. (2005). RelA repression of RelB activity induces selective gene activation downstream of TNF receptors. *Proceedings of the National Academy of Sciences of USA, 102*, 14635–14640.

Klose, R. J., Sarraf, S. A., Schmiedeberg, L., McDermott, S. M., Stancheva, I., & Bird, A. P. (2005). DNA binding selectivity of MeCP2 due to a requirement for A/T sequences adjacent to methyl-CpG. *Molecular Cell, 19*, 667–678.

Landén, M., Davidsson, P., Gottfries, C. G., Grenfeldt, B., Stridsberg, M., & Blennow, K. (1999). Reduction of the small synaptic vesicle protein synaptophysin but not the large dense core chromogranins in the left thalamus of subjects with schizophrenia. *Biology of Psychiatry, 46*, 1698–1702.

Lioy, D. T., Garg, S. K., Monaghan, C. E., Raber, J., Foust, K. D., Kaspar, B. K., et al. (2011). A role for glia in the progression of Rett's syndrome. *Nature, 475*, 497–500.

Lyst, M. J., Ekiert, R., Ebert, D. H., Merusi, C., Nowak, J., Selfridge, J., et al. (2013). Rett syndrome mutations abolish the interaction of MeCP2 with the NCoR/SMRT co-repressor. *Nature Neurosciences, 16*, 898–902.

Maezawa, I., Swanberg, S., Harvey, D., LaSalle, J. M., & Jin, L. W. (2009). Rett syndrome astrocytes are abnormal and spread MeCP2 deficiency through gap junctions. *Journal of Neurosciences, 29*, 5051–5061.

Marksteiner, J., Lechner, T., Kaufmann, W. A., Gurka, P., Humpel, C., Nowakowski, C., et al. (2000). Distribution of chromogranin B-like immunoreactivity in the human hippocampus and its changes in Alzheimer's disease. *Acta Neuropathology, 100*, 205–512.

Naka, H., Nakamura, S., Shimazaki, T., & Okano, H. (2008). Requirement for COUP-TFI and II in the temporal specification of neural stem cells in CNS development. *Nature Neurosciences, 11*, 1014–1023.

Nguyen, M. V., Felice, C. A., Du, F., Covey, M. V., Robinson, J. K., Mandel, G., et al. (2013). Oligodendrocyte lineage cells contribute unique features to Rett syndrome neuropathology. *Journal of Neurosciences, 33*, 18764–18774.

Okabe, Y., Takahashi, T., Mitsumasu, C., Kosai, K., Tanaka, E., & Matsuishi, T. (2012). Alterations of gene expression and glutamate clearance in astrocytes derived from an MeCP2-null mouse model of Rett syndrome. *PLoS ONE, 7*, e35354.

Okamura, M., Kudo, H., Wakabayashi, K., Tanaka, T., Nonaka, A., Uchida, A., et al. (2009). COUP-TFII acts downstream of Wnt/beta-catenin signal to silence PPARgamma gene expression and repress adipogenesis. *Proceedings of the National Academy of Sciences of USA, 106*, 5819–5824.

Sadakata, T., Mizoguchi, A., Sato, Y., Katoh-Semba, R., Fukuda, M., Mikoshiba, K., et al. (2004). The secretory granule-associated protein CAPS2 regulates neurotrophin release and cell survival. *Journal of Neurosciences, 24*, 43–52.

Shahbazian, M., Young, J., Yuva-Paylor, L., Spencer, C., Antalffy, B., Noebels, J., et al. (2002). Mice with truncated MeCP2 recapitulate many Rett syndrome features and display hyperacetylation of histone H3. *Neuron, 35*, 243–254.

Williams, E. C., Zhong, X., Mohamed, A., Li, R., Liu, Y., Dong, Q., et al. (2014). Mutant astrocytes differentiated from Rett syndrome patients-specific iPSCs have adverse effects on wild-type neurons. *Human Molecular Genetics, 23*, 2968–2980.

Yasui, D. H., Peddada, S., Bieda, M. C., Vallero, R. O., Hogart, A., Nagarajan, R. P., et al. (2007). Integrated epigenomic analyses of neuronal MeCP2 reveal a role for long-range interaction with active genes. *Proceedings of the National Academy of Sciences of USA, 104*, 19416–19421.

Yasui, D. H., Xu, H., Dunaway, K. W., Lasalle, J. M., Jin, L. W., & Maezawa, I. (2013). MeCP2 modulates gene expression pathways in astrocytes. *Molecular Autism, 4*, 3.